

# Optimization of a gas flow system by Raman flame temperature measurements

---

Lammert Wiersma  
s2155907  
Combustion Technology,  
Rijksuniversiteit Groningen

## Abstract

In one-dimensional methane-air flames, the equivalence ratio ( $\varphi$ ) and outflow velocity are the parameters that influence a flame's properties. It is therefore important that those parameters be monitored well. In this research, 4 methods of determining  $\varphi$  have been compared: an O<sub>2</sub>- and a CH<sub>4</sub>-concentration meter and two sets of 2 mass flow meters (one for methane, one for air). All meters agreed very well about  $\varphi$ , within 5% of each other.

Raman flame temperature measurements pointed out that the  $\varphi$ s measured are, for all meters, close to the real value. Because the systematic error in Raman temperature measurements as a function of  $\varphi$  is unknown, it is impossible to determine which meter is the best one. The graphs obtained confirm that Raman spectroscopy is a good way to measure temperatures within about 60 K, and that all meters perform quite well.

*Keywords:* Raman spectroscopy, Raman temperature measurements, equivalence ratio measurements, gas flow measurements

*The author would like to thank Anatoli Mokhov, Peter Langenkamp and Howard Levinsky for their useful help and feedback.*



## Table of contents

Introduction.....	4
Theory.....	5
Equivalence ratio.....	5
Measuring flows.....	5
Oxygen concentration.....	6
Methane concentration.....	7
Meters.....	7
Alicat.....	7
Bronkhorst.....	8
Maihak.....	9
Near-adiabatic flames.....	9
Raman spectroscopy.....	9
Software.....	11
Experimental setup.....	13
Gas flow system.....	13
Optical system.....	14
Results and discussion.....	16
Errors.....	16
Experimental comparison.....	16
Flame temperature measurements.....	19
Flow speed dependency.....	20
Temperature-based comparison.....	22
Conclusions.....	25
References.....	26
Appendix: conversion factor for Alicat mixture flow measurements.....	27

## Introduction

Burning methane has become very common during the last few decades. Especially in the Netherlands almost all households cook on 'Slochteren gas', which consists of 82% of methane. It is, however, not very well known how the combustion process works. Inside the flame there appear to be many species interacting with each other<sup>[1]</sup>. The existence of specialized journals such as 'Progress in Energy and Combustion Science' and 'Combustion and Flame' shows that there is interest in this field.

But how can flames be investigated? As few as possible parameters are wanted: less factors to control means less possible errors. It is, for instance, important that there is no time dependence: steady flames are favorable. Because of their relative simplicity, premixed laminar flames are a popular research object. When a burner with a porous burner deck is used, the outflow velocity  $v$  is equal over the entire deck. It is then possible to obtain a virtually one-dimensional flame. In a one-dimensional flame, the flame characteristics are equal for every  $x$  and  $y$ , but change with height. When such a flame is obtained, the flame's properties depend only on the equivalence ratio ( $\varphi \propto$  gas-to-air-ratio, see Theory: Equivalence Ratio) and  $v$ .

So it is necessary to measure and regulate the air and methane flows very accurately. Only when  $\varphi$  and  $v$  are well-known, it is possible to compare experimental results with calculations. In this research, this question has been investigated: which of the meters in the laboratory can be used best to measure  $\varphi$  of a mixture of gas and air?

Because for a given  $\varphi$  and  $v$  many flame parameters can be calculated quite precisely, it is possible to verify the accuracy of a  $\varphi$ - and  $v$ -determination by measuring those flame parameters. In particular flame temperature strongly depends upon  $\varphi$  and  $v$ . In this experiment, Raman spectroscopy was used to measure temperature, and thus to verify the accuracy of the equipment.

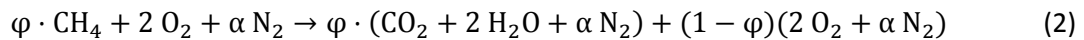
## Theory

### Equivalence ratio

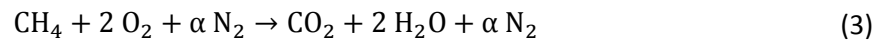
As said before, research in combustion is preferably being done with steady flames in a well-known environment – these are the easiest to investigate. One of the main factors determining the properties of a premixed methane/air flame is the equivalence ratio of the mixture. The composition of a methane-air mixture can be written as



where  $\varphi$  is the equivalence ratio and  $\alpha$  makes sure oxygen and nitrogen react in the right proportions<sup>1</sup>. Generally, it is only possible to ignite a mixture when  $\varphi$  is between 0,5 and 1,5. When  $\varphi < 1$ , the flame is called lean. The reaction is given by:



When  $\varphi$  is 1, the combustion will be complete:



Because complete combustion can take place, a mixture with  $\varphi = 1$  is called stoichiometric. In the case where  $\varphi > 1$  (in 'rich' flames), it is impossible to write a reaction formula. Many partially oxidized species form, making it impossible to fill in coefficients in the reaction equation.

There are three ways of determining the equivalence ratio of a mixture: measuring the gas and air flows, measuring the methane concentration in the mixture and measuring the oxygen concentration in the mixture<sup>2</sup>.

### Measuring flows

Under ordinary circumstances ( $p \sim 1$  bar,  $T \sim 300$  K), the ideal gas law,

$$P \cdot V = N_m \cdot R \cdot T \quad (4)$$

can be used to relate amounts of moles to volumes. In the gas mixture, the pressure and temperature are equal for both air and methane. Therefore, when the ideal gas law for methane ( $P_{\text{CH}_4} \cdot V_{\text{CH}_4} = N_{m,\text{CH}_4} \cdot R \cdot T_{\text{CH}_4}$ ) is divided by the ideal gas law for air ( $P_{\text{air}} \cdot V_{\text{air}} = N_{m,\text{air}} \cdot R \cdot T_{\text{air}}$ ), we obtain

$$\frac{V_{\text{CH}_4}}{V_{\text{air}}} = \frac{N_{\text{CH}_4}}{N_{\text{air}}} = \frac{\varphi}{2 + \alpha} \quad (5)$$

---

<sup>1</sup>In this depiction, air is being regarded as consisting of only oxygen and nitrogen. This is not true – there is also about 1% argon and many trace gases – but those gases are either inert or present only at so small amounts that they can be neglected. Therefore, it is no problem to regard the air as a mixture of oxygen and nitrogen (+other non-reaction gases).  $\alpha + 2$  then is  $\frac{2}{[\text{O}_2]_{\text{air}}}$ , so  $\alpha \approx \frac{2}{0,20947} - 2 = 7,5479$

<sup>2</sup>Of course, it is possible to determine  $\varphi$  by measuring the concentration of any constituent of air. However, the relative amount of air in the mixture only changes by 7% between the richest and the leanest flames. Therefore quite precise concentration measurements of the constituents of air are needed to determine  $\varphi$  with a workable error. In the case of oxygen, this is possible (therefore, we used it). Nitrogen concentrations are harder to measure precisely, and the other constituents ( $\sim 1$  volume%) were not considered in this research.

where the last equality follows from (1). From here, it follows that

$$\left(\frac{V_{CH_4}}{V_{air}}\right)_{stoi} = \frac{1}{2 + \alpha} \quad (6)$$

By dividing eq. (5) by eq. (6),  $\varphi$  can easily be expressed as a function of the gas and air volumes:

$$\varphi = \frac{\left(\frac{V_{CH_4}}{V_{air}}\right)}{\left(\frac{V_{CH_4}}{V_{air}}\right)_{stoi}} = \frac{V_{CH_4}}{V_{air}} \cdot (2 + \alpha) \approx 9,5479 \cdot \frac{V_{CH_4}}{V_{air}} \quad (7)$$

In this experiment, stationary volumes couldn't be measured: only gas flow meters were available.

However, if  $V = Q \cdot \Delta t$  (where  $Q$  = gas flow) is applied in formula (7), we obtain:

$$\varphi \approx 9,5479 \cdot \frac{Q_{CH_4} \cdot \Delta t}{Q_{air} \cdot \Delta t} = 9,5479 \cdot \frac{Q_{CH_4}}{Q_{air}} \quad (8)$$

This is something that can be measured. It would be also useful to be able to predict the magnitude of the error the measurements will give. The most general formula for calculating errors in a function  $f(x_1, \dots, x_n)$  that depends on  $x_1$  to  $x_n$  is:

$$(\delta f(x_1, \dots, x_n))^2 = \left(\frac{\partial f(x_1, \dots, x_n)}{\partial x_1}\right)^2 (\delta x_1)^2 + \dots + \left(\frac{\partial f(x_1, \dots, x_n)}{\partial x_n}\right)^2 (\delta x_n)^2 \quad (9)$$

When  $\varphi$  is determined by measuring  $Q_{CH_4}$  and  $Q_{air}$ ,  $\varphi$  and consequently the error in  $\varphi$  depend on the errors in those gas flows:

$$\begin{aligned} (\delta \varphi)^2 &= \left(\frac{\partial \varphi}{\partial Q_{CH_4}}\right)^2 (\delta Q_{CH_4})^2 + \left(\frac{\partial \varphi}{\partial Q_{air}}\right)^2 (\delta Q_{air})^2 \\ &= \left(\frac{2 + \alpha}{Q_{air}}\right)^2 (\delta Q_{CH_4})^2 + \left(\frac{-(2 + \alpha) \cdot Q_{CH_4}}{(Q_{air})^2}\right)^2 (\delta Q_{air})^2 \\ &= \frac{(2 + \alpha)^2}{(Q_{air})^2} \left[ (\delta Q_{CH_4})^2 + \left(\frac{Q_{CH_4}}{Q_{air}}\right)^2 (\delta Q_{air})^2 \right] \rightarrow \\ \delta \varphi &= \frac{2 + \alpha}{Q_{air}} \sqrt{(\delta Q_{CH_4})^2 + \left(\frac{\varphi}{2 + \alpha}\right)^2 (\delta Q_{air})^2} \quad (10) \end{aligned}$$

### Oxygen concentration

When  $\varphi$  changes, different proportions of air and gas arise, so the oxygen concentration changes.

Quantitatively, the oxygen concentration in the mixture is given by (from (1)):

$$[O_2] = \frac{2}{2 + \varphi + \alpha} \quad (11)$$

$\varphi$  can now be expressed as a function of  $[O_2]$ :

$$(2 + \alpha) \cdot [O_2] + \varphi \cdot [O_2] = 2 \rightarrow \varphi = \frac{2}{[O_2]} - (2 + \alpha) \quad (12)$$

When  $\varphi$  is measured via  $[O_2]$ -measurements, the error  $\delta \varphi$  can directly be related to the error in the  $[O_2]$ -measurements,  $\delta [O_2]$ :

$$(\delta\varphi)^2 = \left(\frac{\partial\varphi}{\partial[O_2]}\right)^2 (\delta[O_2])^2 = \left(-\frac{2}{[O_2]^2}\right)^2 (\delta[O_2])^2 = \frac{4}{[O_2]^4} (\delta[O_2])^2 \rightarrow \delta\varphi = \frac{2}{[O_2]^2} \cdot \delta[O_2] \quad (13)$$

### Methane concentration

When  $\varphi$  changes, the methane concentration of course changes too. So  $[CH_4]$ -measurements can be used to determine  $\varphi$ . The methane concentration in the mixture can be determined from (1):

$$[CH_4] = \frac{\varphi}{2 + \varphi + \alpha} \quad (14)$$

Now, let's rewrite  $\varphi$  in terms of  $[CH_4]$ :

$$(2 + \alpha) \cdot [CH_4] + \varphi \cdot [CH_4] = \varphi \rightarrow \varphi \cdot (1 - [CH_4]) = (2 + \alpha) \cdot [CH_4] \rightarrow \varphi = \frac{(2+\alpha) \cdot [CH_4]}{1 - [CH_4]} \quad (15)$$

The error in  $\varphi$  now depends on the error in  $[CH_4]$ -measurements,  $\delta[CH_4]$ :

$$\begin{aligned} (\delta\varphi)^2 &= \left(\frac{\partial\varphi}{\partial[CH_4]}\right)^2 (\delta[CH_4])^2 = \left(\frac{(1 - [CH_4]) \cdot (2 + \alpha) - (2 + \alpha) \cdot [CH_4] \cdot (-1)}{(1 - [CH_4])^2}\right)^2 (\delta[CH_4])^2 \\ &= \left(\frac{2 + \alpha}{(1 - [CH_4])^2}\right)^2 (\delta[CH_4])^2 \rightarrow \delta\varphi = \frac{2 + \alpha}{(1 - [CH_4])^2} \cdot \delta[CH_4] \end{aligned} \quad (16)$$

### Meters

In the experiment,  $Q_{air}$  and  $Q_{CH_4}$  each are measured with two mass flow meters, an Alicat Scientific flow controller and a Bronkhorst EL-FLOW® flow meter. Both meters use different principles to measure the flow rate.

#### Alicat<sup>[2]</sup>

The Alicat flow controllers use a 'laminar flow element', through which the flow is forced. On both sides of the element the differential pressure is measured, and from the pressure drop the mass flow can be calculated. In laminar, orderly flow, to wit, the mass flow is proportional to the pressure drop over a restriction. The Poiseuille Equation gives a quantitative description of the flow:

$$Q_v = \frac{(P_1 - P_2)\pi r^4}{8\eta L} \quad (17)$$

where  $Q_v$  is the volumetric flow rate,  $P_1$  is the static pressure at the inlet,  $P_2$  is the static pressure at the outlet,  $r$  is the radius of the restriction,  $\eta$  is the absolute viscosity of the fluid and  $L$  is the length of the restriction. In this formula  $\pi$ ,  $r$  and  $L$  are constant, so it can be rewritten as:

$$Q_v = K \left(\frac{\Delta P}{\eta}\right) \quad (18)$$

One might think: how is this a mass flow controller instead of a volumetric flow controller? Well, although the pressure drop ( $\propto$  volumetric flow) is measured, it is – using the ideal gas law, eq. (4) – being converted to volumes at Standard Temperature and Pressure (STP, by Alicat defined as  $T = 298$  K and  $p = 1013,2$  hPa). Thence the flow rates given are only dependent on the amount of gas that passes by, and not on the pressure and temperature in the system.

A controller can be set to a certain gas. When the settings are right, the controller uses the right  $\eta$  and the 'true' flow will be measured. But when a gas or a mixture with a different viscosity is sent through a flow meter, a conversion factor has to be calculated. For the viscosity of a mixture of two gases<sup>[3]</sup>:

$$\eta_m = \frac{\eta_1}{1 + \frac{x_2}{x_1} \Phi_{12}} + \frac{\eta_2}{1 + \frac{x_1}{x_2} \Phi_{21}} \quad (19)$$

Where  $\eta_m$  is the viscosity of the mixture,  $\eta_i$  is the viscosity of a pure component of the mixture at the pressure and temperature of the mixture,  $x$  is the mole fraction of a component in the mixture and  $\Phi_{ij}$  is given by

$$\Phi_{ij} = \frac{\left[ 1 + \left( \frac{\eta_i}{\eta_j} \right)^{\frac{1}{2}} \left( \frac{M_j}{M_i} \right)^{\frac{1}{2}} \right]^2}{\left( \frac{4}{\sqrt{2}} \right) \left[ 1 + \left( \frac{M_i}{M_j} \right)^{\frac{1}{2}} \right]} \quad (20)$$

where  $M_i$  is the molecular weight of a component. In our experiment, one meter that thinks he measures air will have to control a methane-air mixture, so we will calculate a conversion factor to find the true flow rate. Therefore we'll calculate the viscosity of a mixture as a function of  $\varphi$ . First we'll calculate  $\Phi_{12}$  and  $\Phi_{21}$ , where 1 stands for air and 2 for methane. The pure viscosities at  $T = 298$  K are taken from [2]:  $\eta_{air} = 184,332 \mu Poise$ ,  $\eta_{CH_4} = 111,296 \mu Poise$ .  $M_{air} = 28,97 g/mol$ ,  $M_{CH_4} = 16,044 g/mol$ . It turns out that  $\Phi_{12} = 0,808989$  and  $\Phi_{21} = 1,18516$ . In a methane-air mixture,  $\frac{x_1}{x_2} = \frac{2+\alpha}{\varphi}$  (see (1)) so that

$$\eta_m = \frac{\eta_{air}}{1 + \frac{\varphi}{2+\alpha} \Phi_{12}} + \frac{\eta_{CH_4}}{1 + \frac{2+\alpha}{\varphi} \Phi_{21}} = \frac{\eta_{air} \cdot (2+\alpha)}{2+\alpha + \varphi \Phi_{12}} + \frac{\eta_{CH_4} \cdot \varphi}{1 + (2+\alpha) \Phi_{21}} \quad (21)$$

The conversion factors needed  $\left( \frac{\eta_{air}}{\eta_m} \right)$  have been computed for all  $\varphi$  where will be measured and are given in Appendix 1.

### Bronkhorst<sup>[4]</sup>

The Bronkhorst flow meters use another principle: a known fraction of the flow is sent through a capillary tube where the gas is heated. There are two temperature sensors, one upstream and one downstream. The temperature sensors are in a bridge circuit and the imbalance is linearized and amplified, so that the signal is proportional to the temperature difference.  $\Delta T$  can be related to the mass flow: high mass flows result in less energy transfer per unit mass, so a smaller temperature difference. The functional dependence of  $V$  on  $c_p$  and  $Q$  is given by

$$V_{signal} = K \cdot c_p \cdot Q_m = K \cdot c_p \cdot \rho \cdot Q_v \quad (22)$$

where  $K$  is a constant,  $c_p$  is the specific heat of the gas and  $Q_m$  is the mass flow.  $\rho$  is the density of the gas and  $Q_v$  is the volume flow. The meter monitor the temperature and pressure, calculate  $\rho$  and so compensate for pressure and temperature differences. The output of the meters is the flow rate in 'normal' liters per minute. Normal here means at  $T = 273$  K and  $p = 1013,25$  hPa.

To be able to compare readings of the Alicats with readings of the Bronkhorsts, a conversion factor has to be calculated. The conversion factor then from the Bronkhorst values to  $T = 298 \text{ K}, p = 1013,2 \text{ hPa}$  is, using the ideal gas law, (4):  $c = \frac{T_2}{T_1} = \frac{298}{273} = 1,09$ .

### Maihak<sup>[5]</sup>

CH<sub>4</sub>-concentration measurements were done using a Maihak UNOR module. This module uses a non-dispersive infrared (NDIR) sensor: infrared light within an absorption band of methane but not absorbed by other gases is sent through the mixture. Some of it will be absorbed by the methane. The light that hasn't been absorbed falls on a light sensor. The higher the CH<sub>4</sub>-concentration, the less light will reach the sensor. So the light intensity measured by the sensor is a measure for the CH<sub>4</sub>-concentration.

To measure the oxygen concentration, a Maihak OXOR-P module was used. It consists of a rotating diamagnetic dumbbell, suspended in an inhomogeneous magnetic field. Oxygen molecules are paramagnetic, so they will exert a torque on the dumbbell. The more oxygen there is, the greater the torque. This way the module determines the oxygen concentration.

### Near-adiabatic flames

The importance of the equivalence ratio is obvious, but how does  $v$  influence the flame's properties so strongly? Well, when the flame propagation speed  $v_{flame}$  is higher than the outflow speed  $v$ , the flame wants to go into the burner. The porous burner deck prevents the flame from eating in, and consequently the flame 'lies' on top of the burner; this results in much heat loss to the (cool) burner. Higher  $v$  lets the flame lie less on the burner, resulting in less heat loss to the burner. When  $v$  approximates the flame propagation speed, the flame hovers above the burner, and heat loss to the burner is minimal. In fact, upward of  $v$  a little under  $v_{flame}$  (it is surely possible to maintain a flame when  $v$  is not too much higher than  $v_{flame}$ ), the heat loss to the burner is very small and almost constant. In this regime, the flame is called 'near-adiabatic', because there is only little heat loss<sup>3</sup> (footnote:). Then, small changes in the flow speed don't result in large changes of other properties anymore, diminishing the influence of small errors in  $v$ .

### Raman spectroscopy

One of the possible interactions of electromagnetic radiation with matter is the excitation of a molecule by a photon. The molecule, then, can fall back under emission of a photon (there are more possibilities, but this is the one of our interest). When it falls back to its initial state, the process is called Rayleigh scattering. But when it falls back to another state than the initial state, the process is called Raman scattering. The excited photon thus has a wavelength other than the absorbed one. When the final state is higher than the initial one, the radiation is called Stokes radiation. When the final state is lower (so the initial state wasn't the ground state) the radiation is called anti-Stokes radiation. When the intensity of the exciting beam is high enough, there doesn't have to be a real upper level where the molecules are excited to. A so-called *virtual* state can serve as the intermediate step between excitation and de-excitation. Because the molecule in the virtual state possesses an actually forbidden energy, the lifetime of this state is very short.

---

<sup>3</sup> A process is adiabatic when there is no transfer of heat or matter with the surroundings. Close to the burner deck, heat loss to the burner is the dominant loss factor, so when this is minimalized, the flame can there be called near-adiabatic. Higher mixing with the surroundings can take place, so the near-adiabatic approximation doesn't apply to the entire flame.

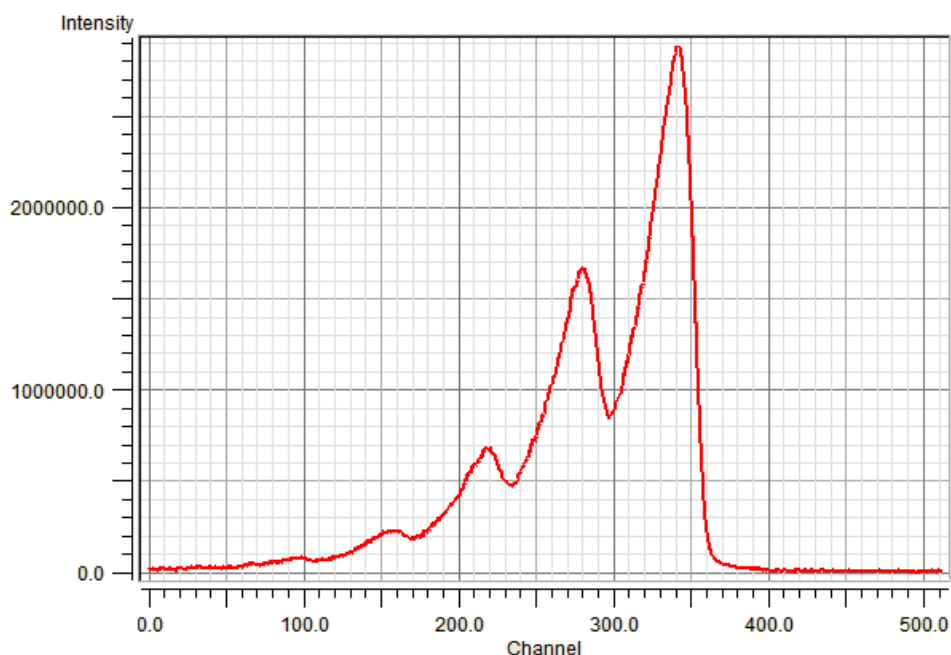
There are different kinds of Raman scattering: overall, a molecule must end up in a different state than the initial one (that's the definition of Raman scattering), but it is not defined of what kind the difference is. Either the vibrational quantum number  $\nu$  or the rotational quantum number  $J$  may change, or both – although the change has to follow certain selection rules. Nitrogen, for instance, can only have  $\Delta\nu = 0, \pm 1$ , where  $\Delta\nu = 0$  either is Rayleigh scattering (when  $\Delta J = 0$ ) or pure rotational Raman scattering. When both change, the process is called 'ro-vibrational Raman scattering'. Changes in  $J$ , however, only have little effect on the energy shift and thus on the wavelength. When a spectrum of scattered wavelengths is recorded, these can therefore be considered as 'fine structure' on the shape of the vibrational spectrum. This is also the reason why pure rotational Raman spectroscopy is not used in this experiment: although the cross-section for rotational Raman scattering is a few orders higher than that for vibrational Raman scattering, the spectral lines are very close to the line of the exciting laser beam. Therefore there is far too much noise to make useful measurements, unless special measures are taken.

Both Stokes- and anti-Stokes scattering is proportional to the population of the initial states, which is proportional to the Boltzmann factor,

$$N_i \propto e^{-\frac{E_i}{k_B T}} \quad (23)$$

where  $k_B$  is the Boltzmann constant. The energy gap between the vibrational levels is large, so even at flame temperatures higher vibrational levels are not densely populated. Therefore, anti-Stokes scattering occurs much less frequently than Stokes-scattering (remember: the initial state for anti-Stokes Raman scattering can't be the ground state). Vibrational Stokes Raman spectroscopy will thus be used.

But why do we want to do Raman spectroscopy at all? Well, as said before, the population of a level is proportional to the Boltzmann factor, (23). So when the temperature rises, the levels with higher energy become more populated. The levels are not equally spaced, so scattering with  $\Delta\nu = +1$



Picture 1. An example of a ro-vibrational Raman spectrum of nitrogen. In fact, the rotational part is not visible. This spectrum has been recorded from a flame with  $\varphi = 1,1$ , and the background is already subtracted (see Experimental Setup)

(vibrational Stokes radiation) occurs at different wavelengths. The relative intensity of Raman-scattered photons with certain wavelengths thus depends on the temperature. Therefore, these intensities can be used to measure temperature. An example of a spectrum is given in Picture 1. According to [6], the temperatures determined with Raman spectroscopy are up to about 60K lower than the real temperatures at  $\varphi = 1,0$ .

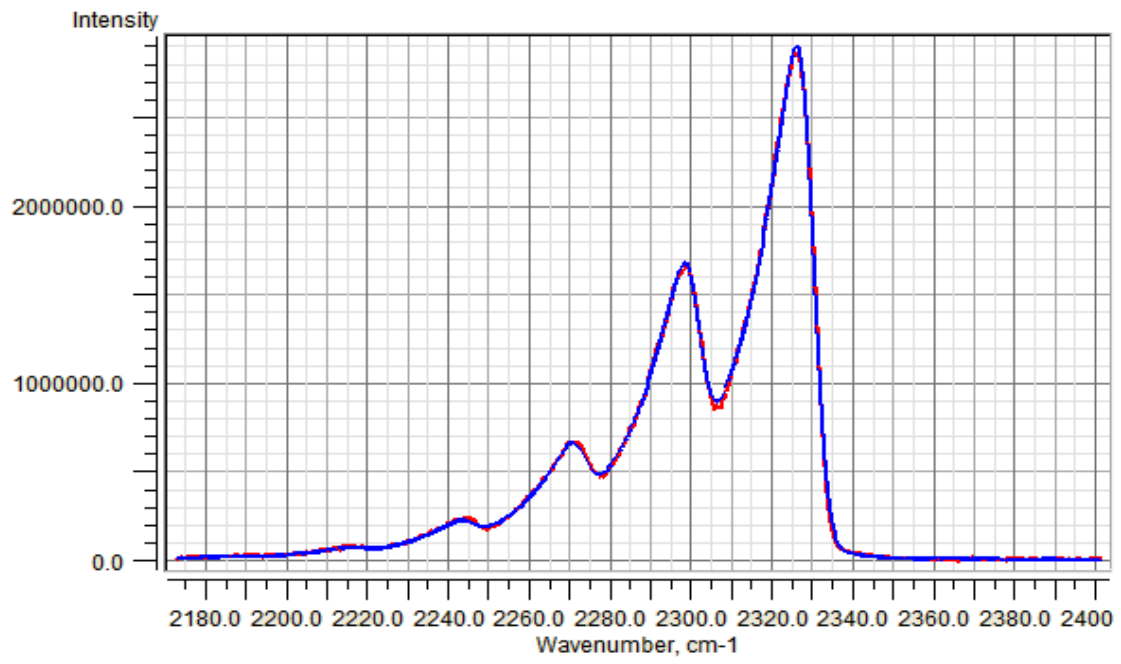
When the exciting beam is polarized, as laser beams are, the emitted photon has the largest probability to be emitted in the plane spanned by the direction of the beam and the vector perpendicular on both the beam and the polarization. There is an easy, classical, explanation for that: suppose the beam is vertically polarized; the photons then induce a vertical electrical field oscillation in the molecule. Viewed from the side, there is a large induced oscillation. Thus emission of a photon in that direction is very probable. Viewed from above, there seems to be no oscillation. Therefore, no photons will be emitted in the plane spanned by the laser beam and the polarization vector. Yet, there are some Raman scattered photons that go there. This is due to the molecular polarizability anisotropy, but this is, because emission in that direction is so weak, not of great importance for our experiments.

## Software

The relative intensities of Raman scattered photons with different wavelengths (the peaks in picture 1) are only a function of the temperature. So it is possible to determine, from those peak heights, the temperature. A program, RamanFit, has been written to determine the temperature, given a spectrum. In advance, the program needs to know the line width of the setup. This can be determined via a spectrum of cold  $N_2$  at room temperature. The linear and quadratic dispersion of the spectrometer can be determined via a spectrum of hot gases, where the peaks are situated at well-known wavelengths. The program determines the temperature by fitting  $T$ . [6] gives a detailed description of the program's working principle. An example of a fit is given in Picture 2.

It is possible to calculate the temperature of a mixture with equivalence ratio  $\varphi$  when all species have reacted adiabatically and a state of equilibrium has been formed. A program called Tecom was used to do this. From thermodynamic data and an equivalence ratio it calculates the temperature and the composition of the gas after equilibrium has been reached adiabatically.

A more complex program, Flameburner, was used to calculate  $v_{flame}$  in different mixtures given  $\varphi$ . Flameburner sets up a grid and tries to solve all equations (conservation of mass, energy, species and the equation of state) among the grid points. A complete description of the working principle of Flameburner is given in [7] and [8].



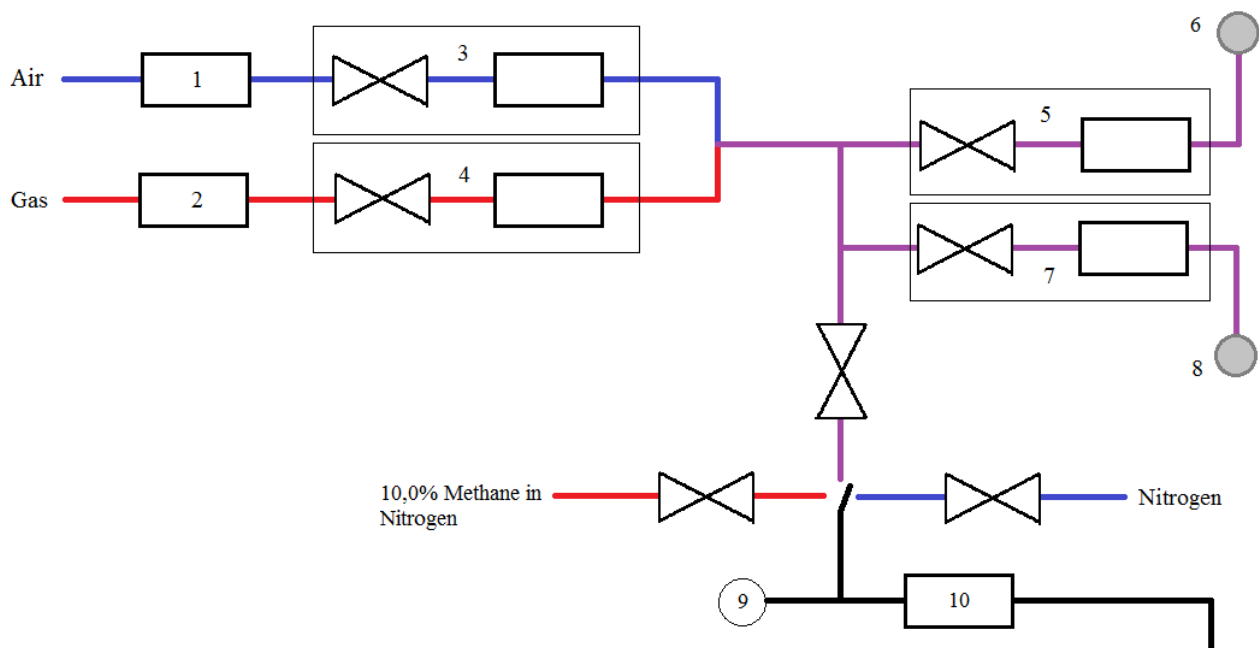
Picture 2. The spectrum of Picture 1 has now been fitted. According to RamanFit, the temperature in this flame was 2154 K. This is about 60 K lower than the adiabatic temperature of a flame with  $\varphi = 1,1$ , which is in accordance with previous experiments that used this method to determine flame temperatures<sup>[6]</sup>

## Experimental setup

### Gas flow system

The gas flow system starts with air and gas inlets. The flow through each pipe is monitored by a Bronkhorst Hi-Tec mass flow meter. The air flow meter (1 in Picture 3) is an EL-FLOW® F-112AC air mass flow meter, the methane flow meter (2) is an EL-FLOW® F-111C methane mass flow meter. Then both gases pass an Alicat Scientific Flow Controller: (3) is an MC-100SLPM-D, (4) is an MC-10SLPM-D (CH<sub>4</sub>). (5) is an Alicat Scientific pressure controller (PC-100PSIG-D), keeping the pressure in the system stable. Excess gas is sent to the bypass burner (6). The flow that goes to the main burner (8) – to be referred to as Total Mass Flow (TMF) – is controlled via an Alicat Scientific mass flow controller (7, MC-100SLPM-D). This construction has been built to enable the experimenter to keep the equivalence ratio perfectly fixed while the outflow velocity can be varied. And it makes it possible to vary the equivalence ratio by adjusting the value of only one of the flow controllers, not both, while the outflow velocity stays constant. This unfortunately didn't work for us in all cases: around  $\varphi = 1$  high flow rates were needed to obtain near-adiabatic flames, and to obtain a high TMF high individual flow rates are needed too. For getting  $\varphi = 1,4$  and  $\varphi = 1,45$  the methane flow rate should have been larger than the meter could let pass, so the air flow rate had to be lowered. Fixing the methane flow rate and varying  $\varphi$  by varying  $Q_{air}$  would not have made it better, because the air flow rate would have needed to be too high for low  $\varphi$ .

The burner is a McKenna products burner with a diameter of 6 cm that has been cooled to keep the burner temperature, and thus the heat flow to the burner, steady. The pressure on the other side of the valve central in the picture can be read with a MONOX D125 (9). (10) is a Sick Maihak S710 hub with an OXOR-P module for [O<sub>2</sub>]-measurement and a UNOR module for [CH<sub>4</sub>]-measurements. This device can be calibrated using the other gases that can be sent to it.



Picture 3. The gas flow part of the system. 1 and 2: Bronkhorst flow meters; 3 and 4: Alicat Scientific flow controllers; 5: Alicat Scientific pressure controller; 6: bypass burner; 7: Alicat Scientific flow controller; 8: main burner; 9: pressure meter; 10: Maihak [O<sub>2</sub>]- and [CH<sub>4</sub>]-meter. The exact types are given in the text;

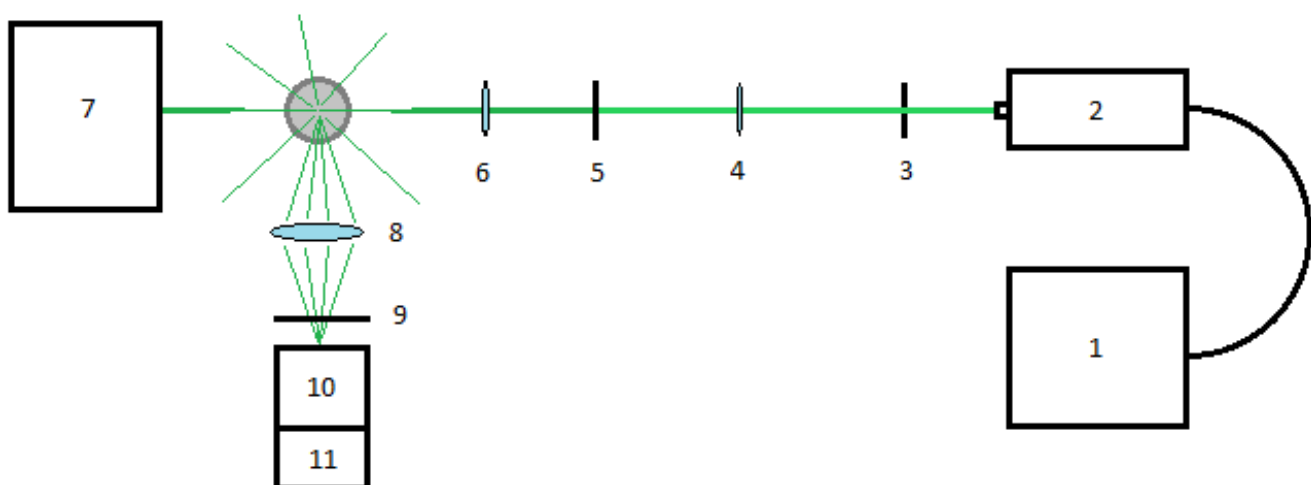
All flow and pressure controllers, Bronkhorst mass flow meters and Maihak S710 are controlled and read via a computer.

On every day when it would be used the Maihak was calibrated with pure Nitrogen, 10,0% methane in nitrogen<sup>4</sup> and compressed air ([O<sub>2</sub>] = 20,947%). The calibration took place with 75 mbar of pressure in the meter, and this pressure was kept constant during all experiments. The other meters were not calibrated.

## Optical system

The optical setup is quite similar to that in [6]. The most important piece of this setup is a Nd:YLF laser (Spectra Physics Empower, 5 kHz repetition rate, 400 ns pulse duration, 30W average power at  $\lambda = 527 \text{ nm}$ ) (2 in Picture 4), controlled via a laser controller (1), which is controlled via a computer. The beam passes a PC-operated shutter (3), to stop the beam without having to shut down the laser. After that, there is a lens (4,  $f = 1200 \text{ mm}$ ) to adjust the beam slightly, and a half-wave plate (5). A half-wave plate is a transparent crystal, cut into a plate, that can change the polarization of light falling in. For a detailed explanation, see for example [9]. The main point now is what it does: when linearly polarized light falls on it, it mirrors this polarization through the plane of one of the crystal's optical axes and the direction of propagation. So when the plate is turned under an angle  $\theta$ , the polarization will rotate by an angle  $2\theta$ . This half-wave plate can be rotated via the computer. Thereafter there is a lens (6,  $f = 500 \text{ mm}$ ), to focus the beam in the center of the flame. The beam passes through the flame and ends up in a beam dump (7).

Perpendicular to the beam there is an  $f/2,8$  lens with focal length 300 mm placed to catch the scattered radiation (8). From this radiation, the Rayleigh-scattered radiation is blocked by a filter (9). The Raman-scattered radiation falls on an  $f/4$  spectrometer (10, Acton Research Spectra Pro 2300i, linear dispersion 2,7 nm/mm), with the entrance slit parallel to the laser beam. The slit width is set at 150  $\mu\text{m}$ . The 2400  $\text{mm}^{-1}$  grating is used. The spectrum is recorded with a PI-Max intensified CCD camera (11, Princeton Instruments, 1024 $\times$ 1024 pixels of 13  $\mu\text{m}$ ). 400 vertical pixels (301-700) are binned, integrating about 10 mm along the laser beam. In all experiments, 2 horizontal pixels are binned. The laser pulses are gated, so that measurement only takes place when the laser gives a



Picture 4. The optical part of the setup. 1: laser controller; 2: Nd:YLF pulsed laser; 3: PC-operated shutter; 4 and 6: lenses to focus the beam on the burner; 5: half-wave plate to adjust the beam polarization; 7: beam dump; 8: lens to focus the scattered light; 9: filter to filter out Rayleigh-scattered light; 10: spectrometer; 11: CCD-camera; the types are given in the text;

pulse. Measuring one spectrum means taking 100 accumulations with 4000 gates per exposure – enough to have no problems with noise. The following is done to minimize the background: always, 2 spectra are recorded. Once with the half-wave plate such that the laser light is not affected, and once with the half-wave plate rotated over  $\pi/4$ . The polarization then changes  $\pi/2$ . Because background radiation mainly comes from reflections and is therefore randomly polarized, its effect should be equal in both spectra. The signal, however, is almost exclusively present in the spectrum from when the laser beam polarization was vertical (see Theory: Raman spectroscopy). When the second spectrum is subtracted from the first one, almost only the signal remains.

On every measurement day, first a room temperature spectrum is recorded. RamanFit needs a spectrum with a well-known temperature to determine the line width of the setup (see Theory: Software).

## Results and discussion

### Errors

As stated under Theory: Meters, all meters have an uncertainty in the measured value. How large this uncertainty is, is taken from literature concerning the respective meters.

- For the Bronkhorst gas flow meters, the uncertainty  $\delta Q$  is 0,5% of the read value (Rd) plus 0,1% of Full Scale (FS)<sup>[4]</sup><sup>5</sup>. The full scale is 109 SLPM for the air flow meter and 10,9 SLPM for the gas meter. So  $(\delta Q_{air})^2 = 0,11^2 + (0,5\% Rd)^2$  SLPM, and  $(\delta Q_{CH_4})^2 = 0,01^2 + (0,5\% Rd)^2$  SLPM. Filling in equation (10):

$$\delta\varphi = \frac{2+\alpha}{Q_{air}} \cdot \sqrt{0,0001 + (0,005 \cdot Q_{CH_4})^2 + \left(\frac{\varphi}{2+\alpha}\right)^2 \cdot (0,0121 + (0,005 \cdot Q_{air})^2)} \quad (24)$$

- The Alicat mass flow meters have an uncertainty of 1% FS<sup>[2]</sup>. Full scale is 100 SLPM for the air flow meter and 10 SLPM for the methane flow meter. Filling in equation (10):

$$\delta\varphi = \frac{2+\alpha}{Q_{air}} \cdot \sqrt{0,01 + \left(\frac{\varphi}{2+\alpha}\right)^2 \cdot 1^2} \quad (25)$$

- The largest contributions to the uncertainty in OXOR-P module measurements come from the linearity deviation (1% FS) and deviations due to pressure changes in the module (<1% per 1% pressure change). All other contributions are very small and can be neglected<sup>[5]</sup>.
- The largest contributions to the uncertainty in the UNOR measurement value come, again, from the linearity deviation (1% FS), and the influence of pressure changes. (0,6-1% change per 1% change in pressure)<sup>[5]</sup>. The pressure has been kept constantly  $75 \pm 0.3$  mbar for both Maihak modules during the experiments, so a pressure change of 0,4% was permitted. The resulting uncertainty thus was maximally  $\sqrt{(1\% FS)^2 + (0,4\% Rd)^2}$  for both modules. All other contributions are very small and can be neglected.

As can be seen in Graph 1, where all relative errors in  $\varphi$  are displayed as a function of  $\varphi$ , the error in  $\varphi$  for [O<sub>2</sub>]-measurements is about four times higher than all other errors. Therefore, the Maihak OXOR-P won't be considered anymore when looking for the best meter. The rise of the Alicat line is due to the fact that for  $\varphi = 1,4$  and  $\varphi = 1,45$   $Q_{air}$  had to be decreased (see Experimental Setup: Gas flow system), while  $\delta Q_{air}$  is independent of  $Q_{air}$  for the Alicat. For the Bronkhorst meters, the lowering of  $Q_{air}$  is compensated by the fact that  $\delta Q_{air}$  is also lowered.

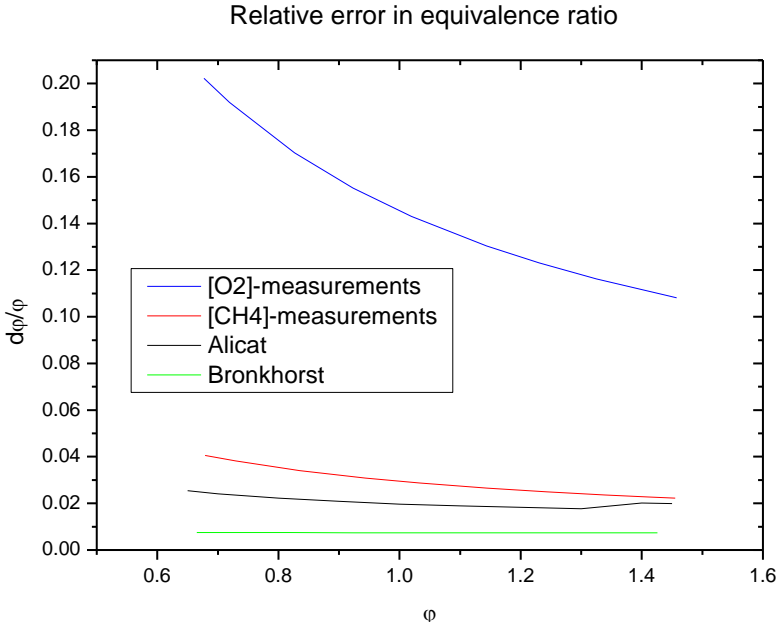
### Experimental comparison

In Graph 2  $\varphi$ -measurements done with the Bronkhorsts, Alicats and [CH<sub>4</sub>]-module are compared. Because the Bronkhorsts theoretically give the lowest error, their  $\varphi$  is on the horizontal axis. It is remarkable that the [CH<sub>4</sub>]-measurements give  $\varphi$  consequently higher than the Bronkhorsts. The Alicats are sometimes higher, sometimes a bit lower. Of course, all meters should give the same value (the black line). For all points, except for one, the theoretical curve falls within its error bars. All three meters agree about  $\varphi$  within 5% over the entire measuring range. This is a good result. However, these points are averages of 5 measurements<sup>6</sup>. The individual measurement points could deviate much more and are plotted in Graph 3. Again, almost all points have their error bars over the theoretical line. There is, though, one measurement day when the measurements of Alicat were

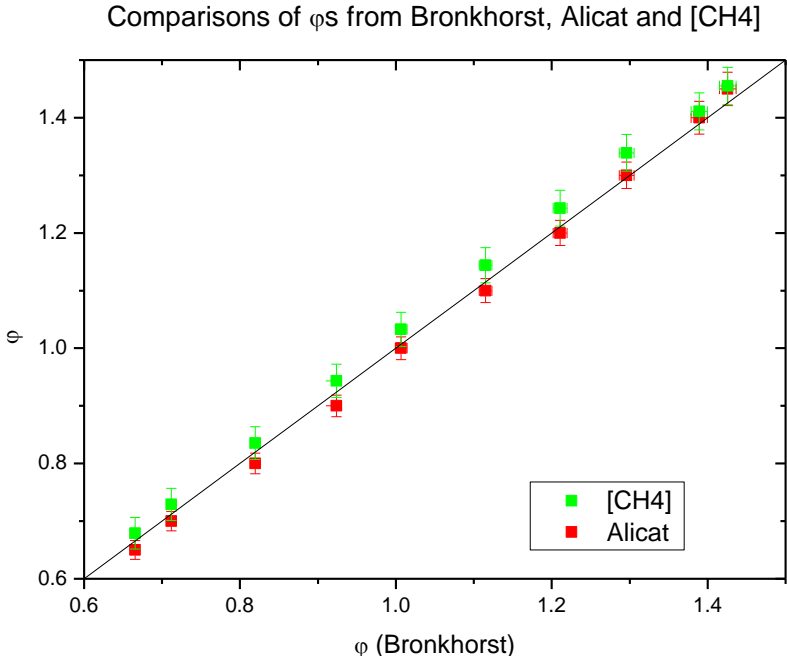
<sup>5</sup> The F-111C is not included in this brochure, but, considering the fact that all meters in the series mentioned have the same uncertainty, the uncertainty is assumed to be the same for the F-111C

<sup>6</sup> 4 for the last two points due to strange Alicat behavior

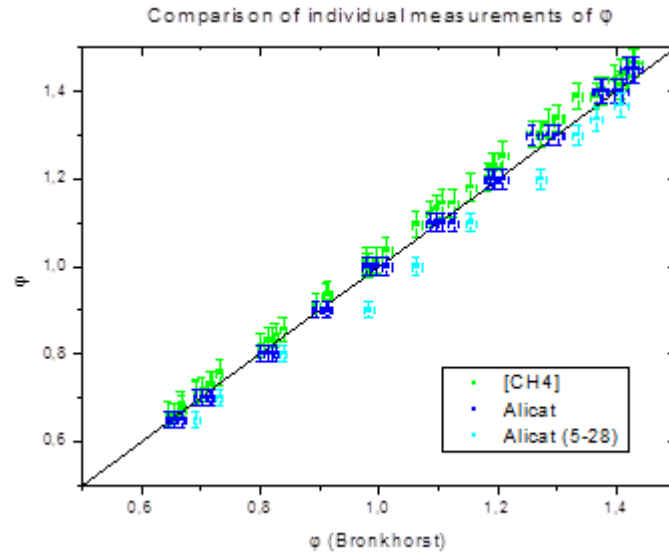
quite different from that of the other meters, with deviations as large as 10%. This came from the Alicat methane flow controller: the Bronkhorst methane flow meter didn't agree with this controller, while the Bronkhorst and Alicat air flow meters agreed very well at this date. This is shown in Graph 4. How this could happen is completely unknown, especially because it only happened on one measuring day, while on all other days this was no problem.



Graph 1. The relative error in  $\phi$  as function of  $\phi$  for the four measurements methods.



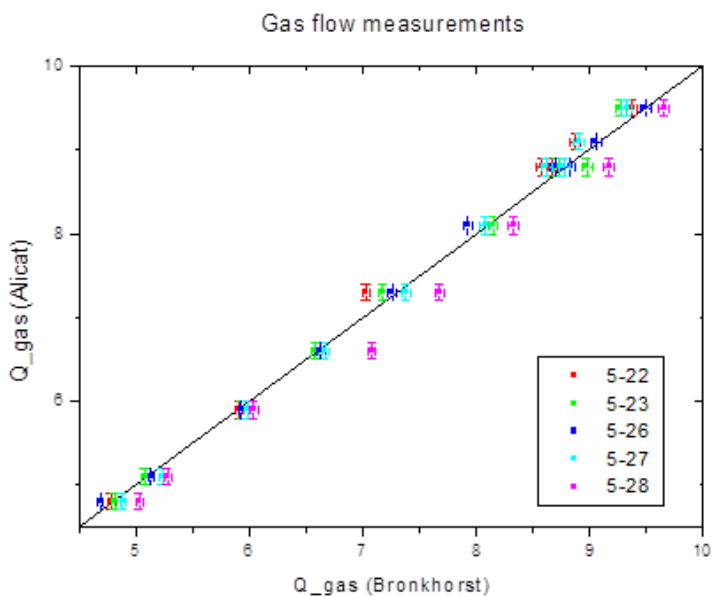
Graph 2. Averaged values of [CH<sub>4</sub>]- Alicat- and Bronkhorst- measurements of  $\phi$  plotted against each other.



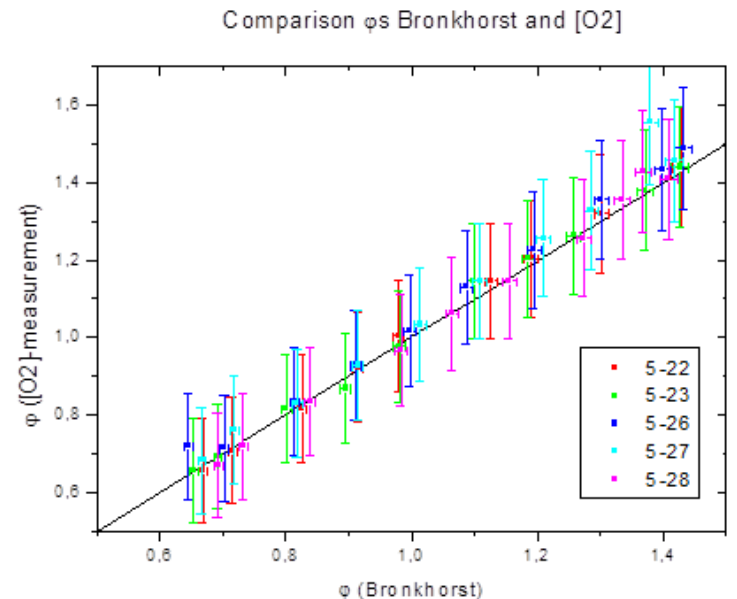
Graph 3. Individual measurement points of  $[CH_4]$ - Alicat- and Bronkhorst- measurements of  $\phi$  plotted against each other.

The overall correspondence of the Bronkhorsts, the Alicats and the  $\phi$ s coming from  $[CH_4]$ - measurements indicates that there are no leaks between the gas flow meters and the point where the air and methane mix. When one of the tubes were leaking, the equivalence ratio according to the  $[CH_4]$ -concentration measurements would be other than given by the gas flow meters.

In Graph 5, the equivalence ratio as measured via the oxygen concentration is plotted against the Bronkhorst values. The  $\phi$  obtained via oxygen concentration measurements is always within 4% of the Bronkhorst values. There is 1 point that deviates largely (measured on 5-27), but this could be failure of the experimenter: sometimes the OXOR-P module gives (wrongly) a very low signal for about 3 seconds. When the concentration has been read exactly in such a dip, this aberrant point could be explained. It would be, however, a large mistake from the experimenter not to recheck the value a bit later. Considering the overall great correspondence between the Bronkhorst and the OXOR-P, it is suggested that the error bars in  $\phi$  ( $[O_2]$ ) are too large.



Graph 4. All measurement points of  $Q_{gas}$  measured by Bronkhorst and Alicat plotted against each other.



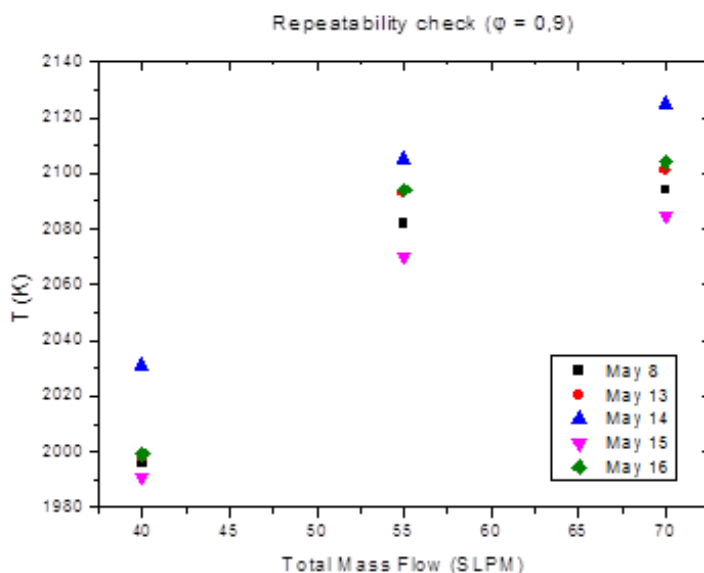
Graph 5. All measurement points of  $\phi$  measured via  $[O_2]$ - measurements plotted against Bronkhorst values

## Flame temperature measurements

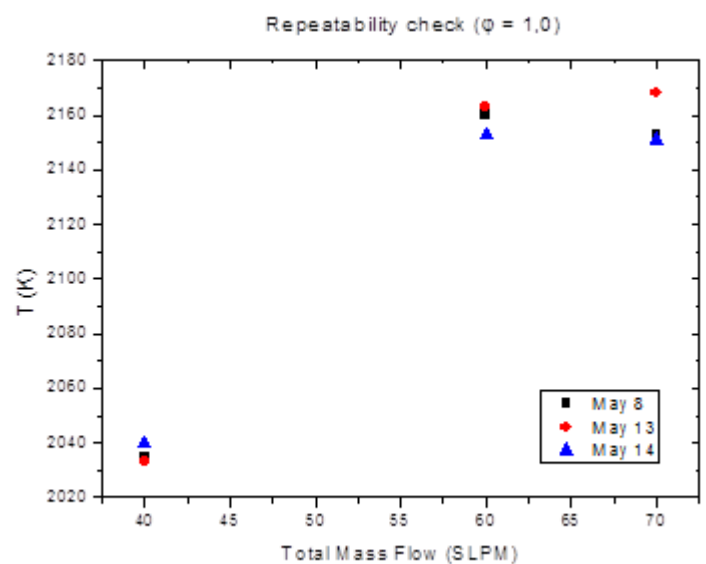
Although the meters correspond very well, do they give the true values for  $\phi$ ? They might all have the same deviation from the true  $\phi$ . To determine whether this is the case, flame temperature measurements have been done at several  $\phi$ s. To measure the temperature,  $N_2$  vibrational Stokes Raman spectra were recorded and the temperature was fitted using the program RamanFit. First, a check has been done to see whether, when on different days equal flames were obtained, temperature measurements yield the same result.

At  $\phi$ s very different from 1, the flame propagation speeds get very low, so the total mass flow (TMF) too and the relative error in TMF becomes larger. Therefore it has been chosen to do the repeatability check at  $\phi = 0,9$  and  $1,0$ . Here, high total flow rates can be used, minimizing the relative error in the TMF.

In graph 6 and 7 the results are shown. The first plan was to measure the temperature on three different days. But the differences at  $\phi=0,9$  were so large that it has been chosen to do measurements for another 2 days. It would have been fairer to do the other 2 measurements for  $\phi=1$  too, because maybe then it would have become clear that the spread in temperature is actually larger than would be thought on the basis of the first three measurements. Besides, 'equal' flames here means: flames with equal settings of the Alicats. Considering the previous graphs, the Alicats aren't the best tools to set really equal flames – the errors of the Bronkhorst flow meters are smaller and they seem to be able to determine  $\phi$  better. Therefore they could have better been used instead of the Alicats.



Graph 6. On several days the temperature of a flame with all settings equal has been measured (here  $\phi = 0,9$ )

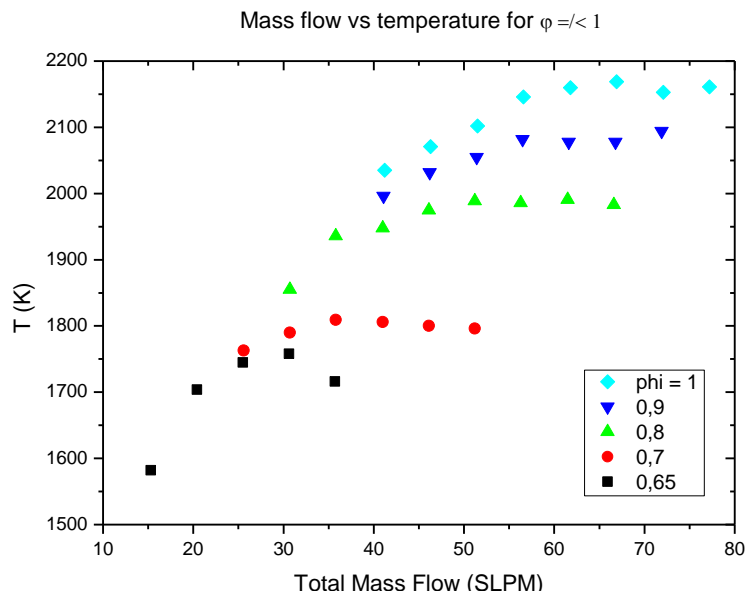


Graph 7. On several days the temperature of a flame with all settings equal has been measured (here  $\phi = 1,0$ )

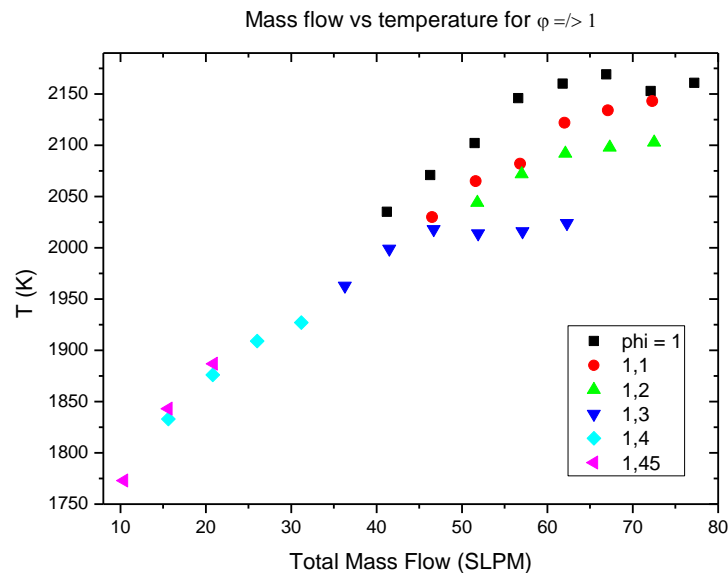
The standard deviation of the points with  $\phi = 0,9$  is 13,7 K, of the points with  $\phi = 1,0$  it is 5,6 K. The method of Raman spectroscopy is expected to have a deviation of the true temperature of about 60K (see Theory), so these deviations are much smaller than that. Therefore it can, despite the fact that the experiment hasn't been done ideally, be concluded that temperature measurements have a good repeatability.

## Flow speed dependency

The next part of the experiment concerned finding the near-adiabatic regime for all  $\varphi$ . It is important that the temperature doesn't change much with varying  $v$ . So at the  $\varphi$ s where would be measured, it was examined how the flow speed influences the flame temperature. In Graph 8 and 9 it can be seen that when the TMF gets higher, the temperature rises. This is due to the fact that at higher  $v$  the heat loss to the burner is reduced. From a certain mass flow the heat loss doesn't change anymore. There the heat loss is minimal and the flame is near-adiabatic. In this regime the flame's temperature should approximate the temperature of an adiabatic flame.

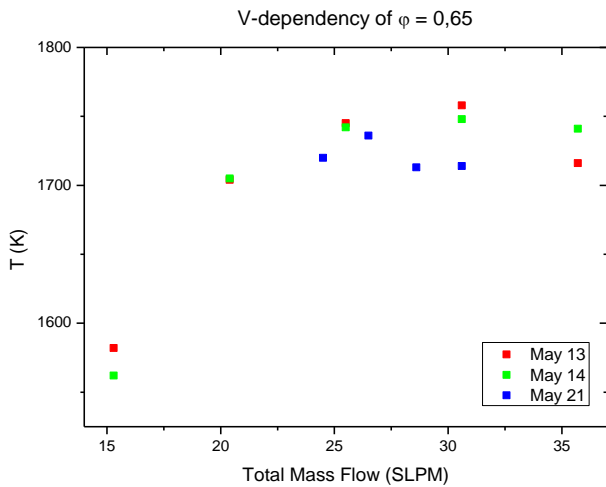


Graph 8. The dependency of the flame's temperature on the mass flow through the burner ( $\varphi \leq 1$ )

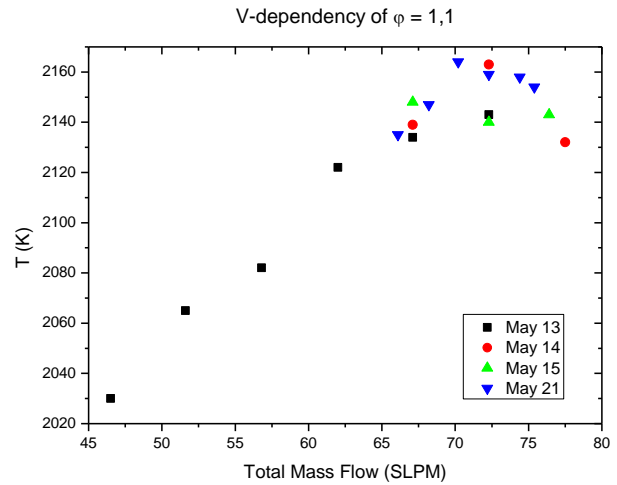


Graph 9. The dependency of the flame's temperature on the mass flow through the burner ( $\varphi \geq 1$ )

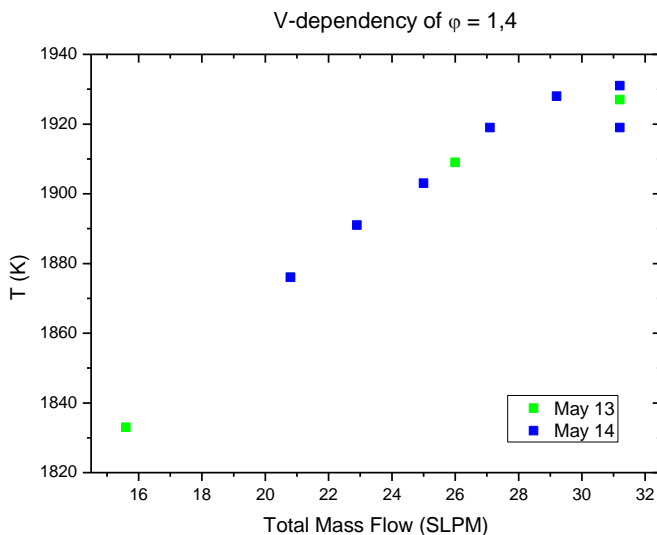
For the graphs that don't become 'flat' more measurements have been done. In Graphs 10 to 13 the results are shown.



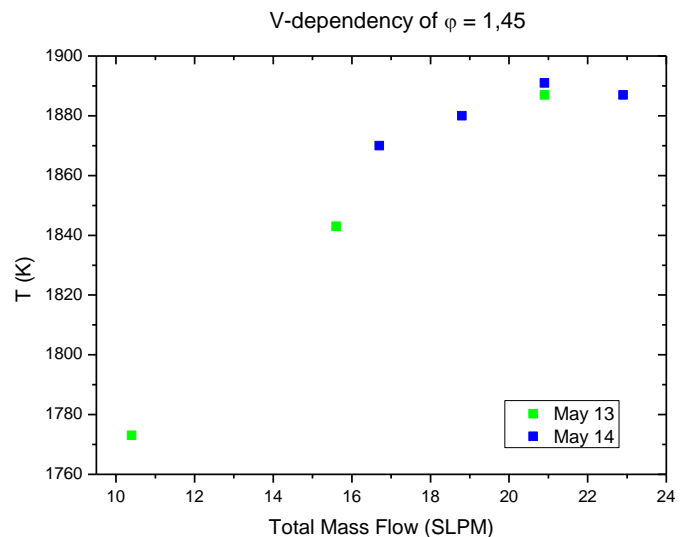
Graph 10. The dependency of the flame's temperature on the mass flow through the burner ( $\phi = 0,65$ )



Graph 11. The dependency of the flame's temperature on the mass flow through the burner ( $\phi = 1,10$ )



Graph 12. The dependency of the flame's temperature on the mass flow through the burner ( $\phi = 1,40$ )



Graph 13. The dependency of the flame's temperature on the mass flow through the burner ( $\phi = 1,45$ )

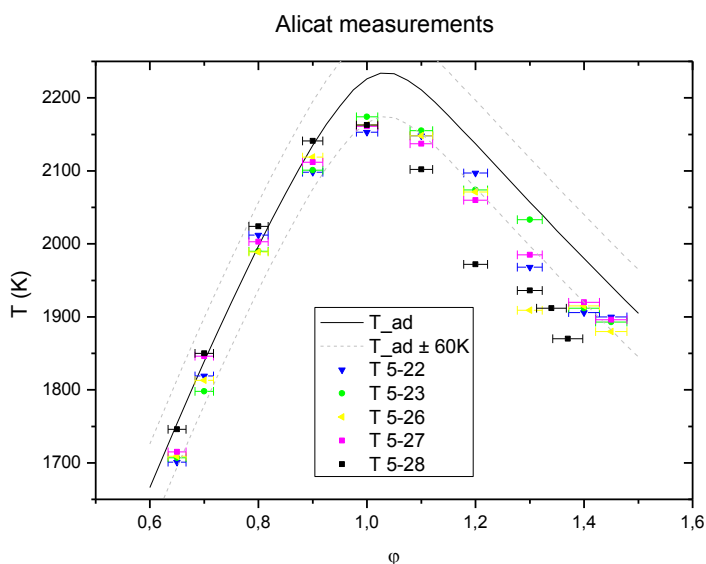
These results – along with observations on flame stability - gave rise to the decision to measure at the flow rates listed in Table 1. In the right column the values are added where theoretically a free flame would be obtained. When there is no value, no Flameburner simulation has succeeded in finding a flame propagation speed. It is remarkable that all values chosen are higher than where a free flame would be expected. This gives us confidence that the flame doesn't rest on the burner anymore, so that it is justified to assume the flame to be near-adiabatic.

$\phi$	Total Mass Flow as set in the flow controller	Obtained Total Mass Flow	Theoretical free flame at
0,65	27	27,5	-
0,70	40	40,9	34,4
0,80	55	56,3	48,6
0,90	60	61,6	60,6
1,00	65	66,9	66,8
1,10	70	72,3	68,7
1,20	65	67,3	61,1
1,30	55	57,1	44,9
1,40	30	31,2	26,1
1,45	21	21,7	-

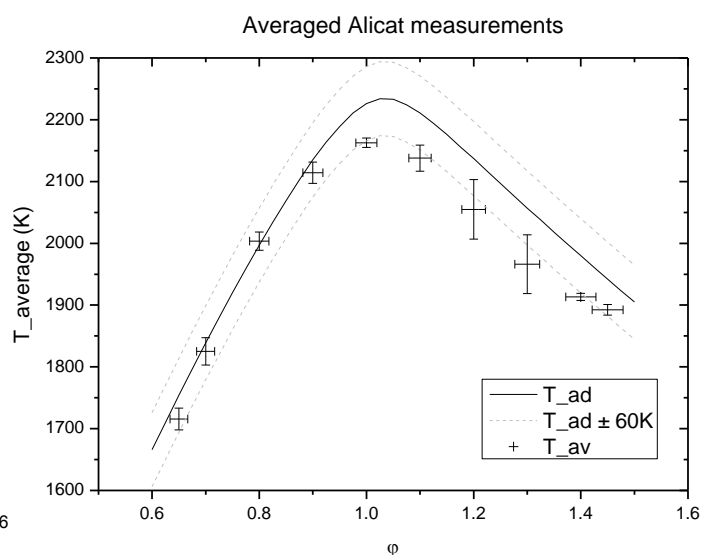
Table 1. Values of the flow rates to set where would be measured alongside with the obtained values (corrected for changes in  $\eta$ ) and flow speeds where theoretically a free flame would be obtained. All mass flows are in SLPM

### Temperature-based comparison

In Graphs 14 and 15 the individual data points and the averaged points of the Alicats are shown. It is not known how the deviation of Raman temperature measurements depends on the temperature. Therefore it is impossible to say from these graphs alone whether the measurements are right or not. The peak of the experimental points should, however, be right under the peak of the theoretical curve. The picture suggests that the measured peak is a bit too far to the lean side, but regarding the error bars it is not possible to say something definite about it. The points for the Bronkhorst

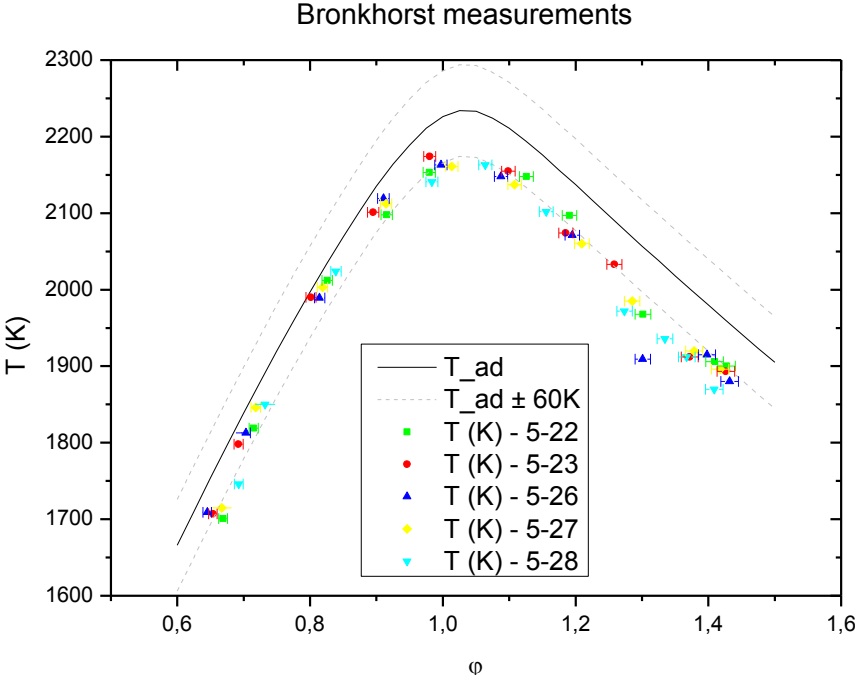


Graph 14. Flame temperature plotted against Alicat flow meter values of  $\phi$ ; the lines  $T_{ad} \pm 60K$  have been added, because the measured  $T_s$  are expected to be 60K lower than de adiabatic temperature.

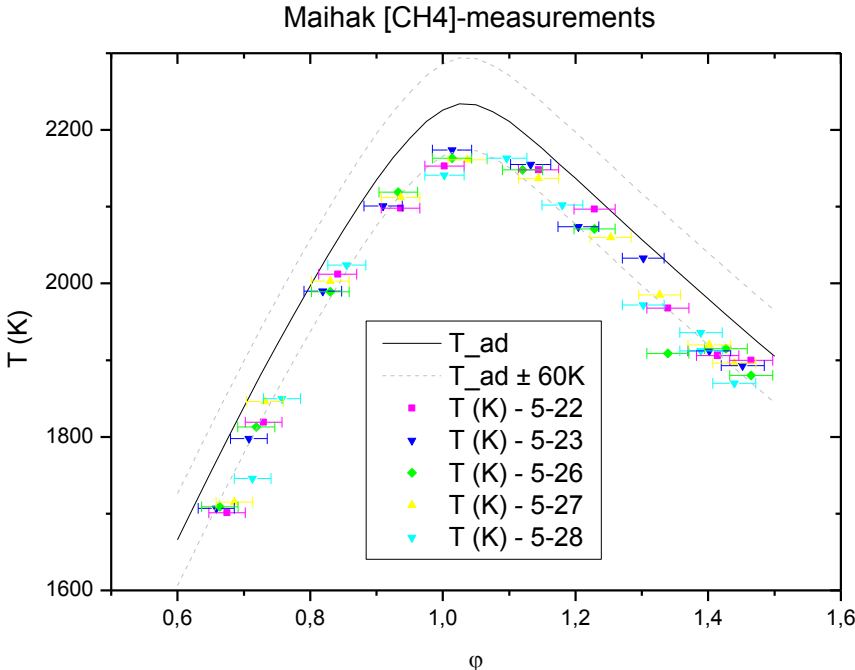


Graph 15. Averaged temperatures at set  $\phi$  with standard deviation in temperature added.

measurements, which would theoretically give the best values, are given in Graph 16. It is known, from the first results, that all meters correspond reasonably well. It is therefore not strange that the graph with Bronkhorst measurements resembles the one with Alicat measurements. Also the graph with [CH<sub>4</sub>]-measurements (Graph 17) resembles the other ones, although this one seems to have less spread.



Graph 16. All data points, with  $\phi$  according to the Bronkhorst mass flow meters. There seems to be less spread than in the Alicat measurements.



Graph 17. The data points, with  $\phi$  according to the Maihak [CH<sub>4</sub>]-meter.

Per measurement type, the standard deviations of the data points from the theoretical curve have been calculated. For completeness, here the [O<sub>2</sub>]-measurements have been taken into account too.

Method	Mean distance under curve (K)	Standard deviation of aberration
Alicat	51,8	40,9
Bronkhorst	60,4	26,4
[O <sub>2</sub> ]	53,2	33,2
[CH <sub>4</sub> ]	59,1	20,7

It can be seen that the points of the [CH<sub>4</sub>]-meter are most evenly spread under the theoretical curve. This could already be seen by eye: over the entire graph the points are around 60 K under the adiabatic curve. This is different in, for example, the Alicat graph. In the left side of that graph the points seem to follow the adiabatic curve perfectly, but the deviations are larger in the right side. From the graphs given is impossible to tell whether the Alicats give very good measurements for lean flames and bad  $\varphi$  for richer flames, or that the [CH<sub>4</sub>]-measurements constantly give the best values. The Bronkhorsts, however, that should give the smallest error, seem to suggest that the truth is somewhere in between.

## Conclusions

During this research it has been studied which meter can be used best when determining the equivalence ratio of a methane-air mixture. In order to obtain an answer it has first been determined how large the theoretical error is in  $\varphi$  for every measurement method. The Bronkhorst mass flow meters theoretically give the smallest errors, but all meters correspond very well with them (usually within 5%). Even  $\varphi$  obtained via  $[O_2]$ -measurements, with a very large expected error, deviated maximally 4%. On one measurement day, the Alicat methane flow controller inexplicably gave values deviating about 10% from what Bronkhorst gave. This puts Alicat in a bad light. The overall good correspondence indicates that there are no leaks in the system and all meters do their job quite well.

To determine whether the meters were right about  $\varphi$  or not, Raman flame temperature measurements have been done. First it has been researched how reproducible temperature measurements are. For  $\varphi = 0,9$  the standard deviation was 13 K, for  $\varphi=1$  it was 6 K, both much lower than the theoretically expected deviation of the Raman temperature measurements from the real temperature (about  $\sim 50K$ ), however  $\varphi$  was set using the Alicats – not the best controller in the lab. Maybe even lower deviations would have been obtained when the Bronkhorst were used instead of the Alicats. But even controlled via the Alicats, the Raman flame temperature measurements have a very good reproducibility.

It has been measured from what total mass flow a near-adiabatic flame was obtained for all  $\varphi$ . This resulted in, for every  $\varphi$ , a flow speed where to measure in future. These flow speeds each resulted in higher  $v$  at the burner than  $v_{flame}$ , which gives an indication there was indeed little heat loss to the burner. At these flow speeds Raman spectra have been recorded, and the measurement values of all meters have been recorded. The temperatures, that were obtained by fitting the spectra with a program, have been plotted against the respective  $\varphi$ s. For all meters a separate plot was made with the adiabatic curve in it too. As expected, the differences in plots obtained for different meters is only small. All curves have their peak about right under the peak of the adiabatic temperature curve, which indicates that the  $\varphi$ s measured are very close to the real ones.

Because all meters measured values so close to each other, and there was no meter that gave obvious bad results, it is from this research impossible to tell which meter is the best one. Only when it is known how the systematic error in Raman temperature measurements varies with  $\varphi$ , conclusions can be drawn about which meter measures  $\varphi$  best. It is suggested that this be researched. More precise results could also be obtained by measurements of for example  $[H_2]$  or  $[CO]$ . In this experiment it has been chosen to use temperature as measured flame parameter, but those parameters depend strongly on  $\varphi$  too.

Apart from the problems giving fine results, it has been seen that the meters agree very well about the equivalence ratio. All meters perform quite well, even the  $O_2$ -meter that theoretically could give large deviations. Besides it has been confirmed that the method used in this research is a reliable way to obtain information about flame temperatures, within a range of about 60 K (4%). Therefore this research boosts the confidence in Raman temperature measurements as well as the confidence in the meters available in the lab. So until further research has been done, the choice for the best meter might be made on the basis of ease-of-use (but don't use the Alicats, they might have a bad day!).

## References

- [1] Warnatz, J., Maas, U., Dibble, R. W. (1996). *Combustion: Physical and Chemical Fundamentals, Modeling and Simulation, Experiments, Pollutant Formation* (4<sup>th</sup> edition). Berlin, Heidelberg, New York: Springer.
- [2] Alicat Scientific (2004). *16 Series: Mass en Volumetric Flow Controllers, Precision Gas Flow Controllers* (Operating Manual). Tucson, AZ: Alicat Scientific, Inc.
- [3] Wilke, C. R. (1950). A Viscosity Equation for Gas Mixtures. *The Journal of Chemical Physics*, 18(4), 517-519.
- [4] Bronkhorst High-Tech (2014). *EL-FLOW®: Digital Thermal Mass Flow Meters and Controllers for Gases* (brochure). Ruurlo: Bronkhorst High-Tech.
- [5] SICK|MAIHAK (2006). *S700 Gas Analyzer: Modular Gas Analyzer System* (Data sheet). Reute, Germany: SICK MAIHAK GmbH.
- [6] Sepman, A. V., Toro, V. V., Mokhov, A. V., Levinsky, H. B. (2013). Determination of temperature and concentrations of main components in flames by fitting measured Raman spectra. *Applied Physics B-lasers and Optics*, 112 (1), 35-47. DOI 10.1007/s00340-013-5389-2.
- [7] Kee, J. K., Grcar, J. F., Miller, J. A., Meeks, E. & Smooke, M. D. (1998). *Premix: a Fortran Program for Modeling Steady Laminar One-Dimensional Premixed Flames*. Premix's user manual. San Diego, CA: Reaction Design.
- [8] Grcar, J. F. (1992). *The Twopnt Program for Boundary Value Problems* (version 3.10). Twopnt's user manual. San Diego, CA: Reaction Design.
- [9] Hecht, E. (2002). *Optics* (4<sup>th</sup> edition). San Fransisco, CA: Addison Wesley.

## Appendix: conversion factor for Alicat mixture flow measurements

$\varphi$	Factor
0,65	1,01978
0,7	1,02126
0,8	1,02418
0,9	1,02708
1,0	1,02996
1,1	1,03281
1,2	1,03563
1,3	1,03842
1,4	1,04120
1,45	1,04257